

Substituent and Noncovalent Interaction Effects in the Reactivity of Purine Derivatives with Tetracarboxylato-dirhodium(II) Units. Rationalization of a Rare Binding Mode via N3

Pilar Amo-Ochoa,^{*,†} Oscar Castillo,[§] Ross W. Harrington,[‡] Félix Zamora,[†] and Andrew Houlton^{*,‡}

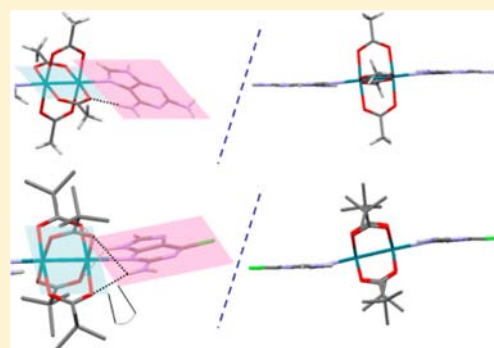
[†]Departamento de Química Inorgánica, Universidad Autónoma de Madrid, 28049 Madrid, Spain

[§]Departamento de Química Inorgánica, Facultad de Ciencia y Tecnología, Universidad del País Vasco (UPV/EHU), Apartado 644, E-48080 Bilbao, Spain

[‡]Chemical Nanoscience Laboratory, School of Chemistry, Newcastle University, Newcastle upon Tyne, NE1 7RU, U.K.

Supporting Information

ABSTRACT: Reactions between $[\text{Rh}_2(\text{CH}_3\text{COO})_4]$ with 2,6-diaminopurine (HDap) or 6-chloro-2-aminopurine (HClap) and $[\text{Rh}_2((\text{CH}_3)_3\text{CCOO})_4]$ with HClap produce three new dirhodium(II) carboxylate complexes of the general form, $[\text{Rh}_2(\text{RCOO})_4(\text{Purine})_2]$ ($\text{R} = \text{CH}_3, (\text{CH}_3)_3\text{C}$). Single crystal X-ray diffraction studies confirm that in all cases the purine coordinates to the axial position of the dirhodium(II)tetracarboxylate unit. However, while the complex obtained with HDap features the typical purine binding mode via N(7), complexes containing HClap show unusual N3 coordination. This is an extremely rare instance of an *unrestricted* purine binding via N3. Some rationalization of these data is offered based on a series of DFT calculations.



INTRODUCTION

Tuning the reactivity of metal centers to display different ligand selectivities and binding modes is a fundamental aspect of coordination chemistry with relevance to metallo-drugs,¹ catalysis² and extraction technologies,^{3,4} etc. This is most effectively achieved when both coordinate and noncovalent interactions are considered. For example, while the reaction of metal-containing antitumor drugs, and related compounds, is dominated by coordinate bond formation with the nucleobases of DNA, noncovalent interactions also play an important role. For example, the 1, 2-intrastrand DNA adduct of *cis-platin* is stabilized by $\text{Pt}-\text{NH}_3 \cdots \text{O}$ hydrogen bonding, and this capacity is frequently retained in newly designed candidates.⁵⁻⁷ The highly selective binding of thymine over the other nucleobases by Zn(II)-cyclen complexes is another example, and this arises from the highly complementary nature of the coordinate and noncovalent bonding (Figure 1).⁸

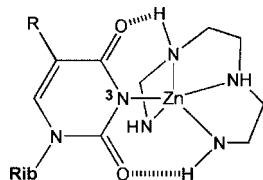


Figure 1. Schematic representation of the selective binding mode of thymine by Zn(II)-cyclen complex.

The tetracarboxylato-dirhodium complexes are another class of compounds whose interactions with nucleobases, first studied 35 years ago,^{9,10} is strongly influenced by such factors.¹¹⁻¹³ Initial interest in these compounds was because $[\text{Rh}_2(\text{CH}_3\text{COO})_4]$ and related compounds, could act as potential antitumor agents with a mechanism of action similar to that exhibited by *cis-platin*.^{14,15}

Early reports on the coordination modes of these dinuclear compounds to DNA showed preferential binding to the adenine rather than guanine.¹⁶ This selectivity was considered to be related to the fact that the dirhodium unit reacts preferentially via *trans*-substitution of the axial ligands (ax) (Figure 2) rather than through the bridging equatorial ones.¹⁷

This has been used to explain the coordination binding modes reported so far for guanine¹⁸ and cytosine¹⁹ bases. The initial studies have suggested that dirhodium-tetracarboxylates do not bind to the preferred N(7)-guanine, N(3)-cytosine, or N(3)-thymine sites through its axial positions.²⁰ This was rationalized by repulsive interactions between the carboxylate oxygen and O(6) of guanine, O(2) of cytosine, and O(2)/O(4) of thymine, respectively, precluding the nucleobase binding to the rhodium center (Figure 2c).²¹ Such arguments are supported by the observation of the typical N7-binding of N9-substituted adenine, in the case of tetrakis(μ -acetato)-bis-(1-methyladenosine)dirhodium(II) monohydrate and bis[(μ_2 -

Received: November 28, 2012

Published: February 1, 2013

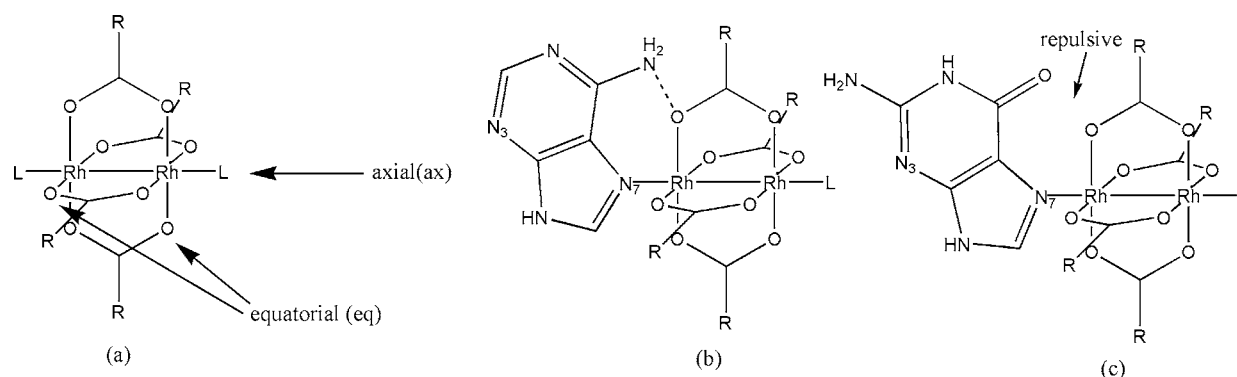


Figure 2. Schematic representation of tetracarboxylatodirhodium units and its two potential substitution sites (a). Interligand interactions of DNA purines with dirhodium(II)tetracarboxylato: attractive interactions with adenine (b) and repulsive interactions with guanine (c).

acetamido)-(μ_2 -trifluoroacetato)-(9-methyladeninium)-rhodium] dinitrate,¹⁶ which features hydrogen bonding between adenine N(6)H₂ and oxygen of carboxylate ligands (Figure 2b).²²

This reactivity pattern can, however, be modified by replacing the carboxylate unit with a bridging group that contains H-donor capability, for example, acetamide. In such cases binding to the typically preferred N(7)-guanine or N(3)-cytosine may be observed, with H-bond formation between the O(6)G or O(2)C and the NH-group of the acetamide.^{16,17}

To further explore these aspects of the chemistry of the dirhodium unit, we have considered reactions with the purine derivatives, 2,6-diaminopurine (HDap) and 6-chloro-2-aminopurine (HClap).²³ These are chosen as they display similarities to the nucleobases, adenine, and guanine. For instance, HClap has the 2-amino group in common with guanine, along with an electron-rich 6-substituent that does not contain protons. On the other hand HDap has a 6-amino function, like adenine, yet contains the same functionalities on the lower, minor groove, edge as in guanine and HClap (namely, 2-amino, N3, N(9)H, see Figure 3). We are particularly interested in the possibility of

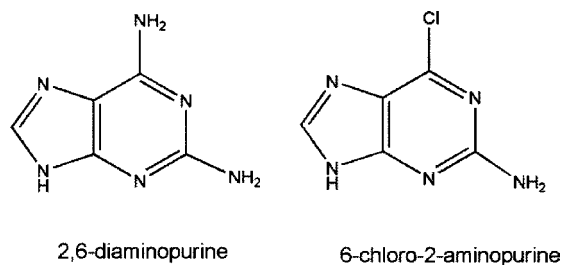


Figure 3. Purines used in this work: 2,6-diaminopurine (HDap) and 6-chloro-2-aminopurine (HClap).

realizing less common binding modes such as at the minor-groove based site, N3. This site is now known to bind to a range of metal ions, though this is generally as a result of additional constraints, such as the presence of steric hindrance at N6^{24–28} or a tethered chelating group at N9.^{29–40} The former examples include that of N3-bound azathiopurine (HAza), to $[\text{Rh}_2(\text{CH}_3\text{COO})_4]$ where the presence of the 6-(1-methyl-4-nitroimidazol-5-yl)thio group is judged to inhibit binding at the more usual purine N1/N7 sites.²⁸

We report here on reactions of the purine derivatives HDap and HClap with the dirhodium-tetracarboxylato species, $[\text{Rh}_2(\text{CH}_3\text{COO})_4]$ and $[\text{Rh}_2((\text{CH}_3)_3\text{CCOO})_4]$, describe sin-

gle-crystal X-ray diffraction studies of the isolated products, and present DFT calculations, which offer some insight into the chemistry.

EXPERIMENTAL SECTION

Materials. $[\text{Rh}_2(\text{CH}_3\text{COO})_4]$, 2,6-diaminopurine, 6-chloro-2-aminopurine, and solvents were purchased and used as received. The $[\text{Rh}_2((\text{CH}_3)_3\text{CCOO})_4(\text{H}_2\text{O})_2]$ complex was obtained by metathesis reaction of tetraacetatodirhodium(II) in excess of trimethylacetic acid, following a similar method to that described by Rempel et al.⁴¹ IR spectra were recorded on a PerkinElmer spectrum 100 spectrophotometer using a universal ATR sampling accessory. Elemental Analyses were carried out by the Microanalytical Service of the Autónoma University of Madrid. L-SIMS spectra were obtained with a Waters/Autospec mass spectrometer, using m-NBA (m-nitrobenzyl alcohol) as matrix. Peak identifications were based on the m/z values and the isotopic distribution patterns. Powder X-ray diffraction has been done using a Diffractometer PANalyticalX'Pert PRO $\theta/2\theta$ primary monochromator and detector with fast X'Celerator. The samples have been analyzed with scanning $\theta/2\theta$.

Synthesis of $[\text{Rh}_2(\text{CH}_3\text{COO})_4(\text{N}7\text{-}2,6\text{-diaminopurine})_2]\cdot 4\text{-}(\text{CH}_3)_2\text{NCHO}$ (1). A mixture of $[\text{Rh}_2(\text{CH}_3\text{COO})_4]$ (0.100 g, 0.226 mmol) and 2,6-diaminopurine (0.074 g, 0.492 mmol) in 16 mL of dimethylformamide (DMF), was stirred at 20 °C for 24 h. The violet solid obtained was filtered off and washed with cold water and dried in air (0.075 g, 37.5% yield of complex 1, based on Rh). Anal. Calcd for $\text{C}_{30}\text{H}_{52}\text{N}_{16}\text{O}_{12}\text{Rh}_2$: C 34.80%, H 5.03%, N 21.67%; found C, 35.01%, H, 4.99%, N, 21.89%. IR selected data (KBr, cm^{-1}): 3397(s), 3140(m), 3002(w), 2823(w), 1672(s), 1649(s), 1589(s), 1490(s), 1408(s), 1255(w), 1239(m), 1106(m), 1093(m), 950(m), 791(w), 7001(w), 664(w), 593(w). ESI-MS: m/z 742 ($[\text{Rh}_2(\text{CH}_3\text{COO})_4(\text{N}7\text{-}2,6\text{-diaminopurine})_2]^+$). The purity of the isolated solid is confirmed by Powder X-ray diffraction that shows only diffraction peaks corresponding to the single crystal.

Synthesis of $[\text{Rh}_2(\text{CH}_3\text{COO})_4(\text{N}3\text{-}6\text{-chloro-}2\text{-aminopurine})_2]\cdot 16\text{H}_2\text{O}$ (2). A mixture of $[\text{Rh}_2(\text{CH}_3\text{COO})_4]$ (0.100 g, 0.226 mmol) and 6-chloro-2-aminopurine (0.068 g, 0.400 mmol) in 16 mL of dimethylformamide (DMF), was stirred at 20 °C for 24 h. The violet solid obtained was filtered off and washed with cold water and dried in air (0.097 g, 59.9% yield of complex 2, based on Rh). Anal. Calcd for $\text{C}_{18}\text{H}_{52}\text{N}_{10}\text{O}_{24}\text{Cl}_2\text{Rh}_2$: C 20.25%, H 4.69%, N 13.12%; found C, 20.87%, H, 4.88%, N, 13.31%. IR selected data (KBr, cm^{-1}): 3374(s), 3192(m), 2926(w), 2850(w), 1675(m), 1649(m), 1591(s), 1562(s), 1423(s), 1307(m), 1259(m), 1095(w), 1042(w), 926 (m), 695(m).). ESI-MS: m/z 611 ($[\text{Rh}_2(\text{CH}_3\text{COO})_4(\text{N}3\text{-}6\text{-chloro-}2\text{-aminopurine})_2]^+$). Powder X-ray diffraction confirms the purity of the isolated solid.

Synthesis of $[\text{Rh}_2((\text{CH}_3)_3\text{CCOO})_4(\text{N}3\text{-}6\text{-chloro-}2\text{-aminopurine})_2]\cdot 2(\text{CH}_3)_2\text{NCHO}$ (3). Compound 3 was obtained analogously to compound 1, using $[\text{Rh}_2((\text{CH}_3)_3\text{CCOO})_4(\text{H}_2\text{O})_2]$ instead of the $[\text{Rh}_2(\text{CH}_3\text{COO})_4]$. The violet solid obtained was

Table 1. Crystallographic Data and Structure Refinement Details of compounds 1–3

	1	2	3
formula	C ₃₀ H ₅₂ N ₁₆ O ₁₂ Rh ₂	C ₁₈ H ₅₂ Cl ₂ N ₁₀ O ₂₄ Rh ₂	C ₃₆ H ₅₈ Cl ₂ N ₁₂ O ₁₀ Rh ₂
formula weight	1034.70	1069.42	1095.66
crystal system	monoclinic	monoclinic	monoclinic
space group	P2 ₁ /c	P2 ₁ /c	P2 ₁
a (Å)	8.1817(2)	11.4531(5)	8.9815(2)
b (Å)	31.4893(6)	22.4591(9)	22.5288(5)
c (Å)	8.2951(2)	8.1567(3)	12.4191(3)
β (deg)	97.415(2)	103.393(4)	108.848(1)
V (Å ³)	2119.24(8)	2041.06(14)	2378.16(9)
Z	2	2	2
T (K)	150(2)	150(2)	296(2)
λ (Å)	1.54178	0.71073	1.54178
ρ _{calcd} (g cm ⁻³)	1.621	1.740	1.530
μ (mm ⁻¹)	6.960	1.034	7.188
reflins collected	15075	10808	27462
unique data/params	3538/280	4693/240	9939/557
R _{int}	0.0321	0.0222	0.0346
GOF (S) ^a	1.052	1.143	1.273
R ₁ ^b /R ₂ ^c [I > 2σ(I)]	0.0246/0.0606	0.0402/0.0809	0.0467/0.1202
R ₁ ^b /R ₂ ^c [all data]	0.0289/0.0619	0.0544/0.0845	0.0594/0.1387

^aS = $[\sum w(F_o^2 - F_c^2)^2 / (N_{obs} - N_{param})]^{1/2}$. ^bR₁ = $\sum ||F_o| - |F_c|| / \sum |F_o|$. ^cR₂ = $[\sum w(F_o^2 - F_c^2)^2 / \sum wF_o^2]^{1/2}$; $w = 1 / [\sigma^2(F_o^2) + (aP)^2 + bP]$ where $P = (\max(F_o^2, 0) + 2F_c^2) / 3$ with $a = 0.0408$ (1), 0.0222 (2), 0.0637 (3) and $b = 0.2547$ (1), 5.6404 (2), 4.3991 (3).

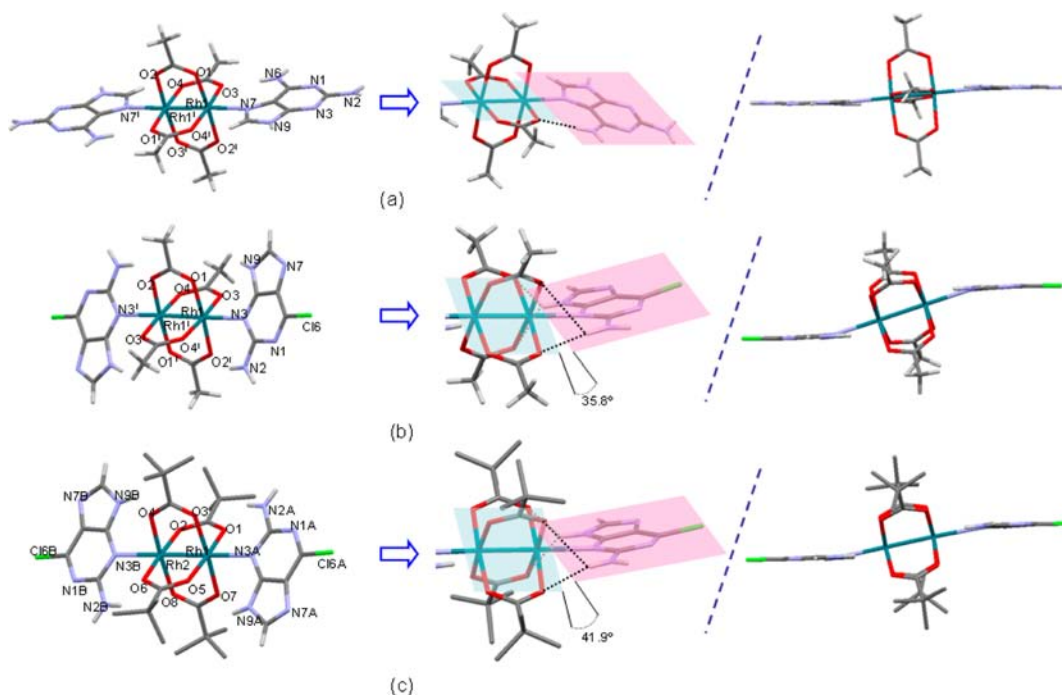


Figure 4. Paddle-wheel shaped dimeric units (left) and intradimeric hydrogen bonding interactions and purine ligand orientation with respect to Rh₂(carboxylate)₂ plane (right) in compounds 1 (a), 2 (b), and 3 (c). For compound 3, the hydrogen atoms of the methyl groups have been omitted for clarity.

filtered off and washed with cold water and dried in air (0.055 g, 64.7% yield of complex 3, based on Rh). Anal. Calcd for C₃₆H₅₈N₁₂O₁₀Cl₂Rh₂: C 39.49%, H 5.30%, N 15.36%; found C, 39.01%, H, 4.96%, N, 15.89%. IR selected data (KBr, cm⁻¹): 3446(s), 3317(s), 3212(s), 2963(w), 2932(w), 1644(s), 1565(s), 1510(m), 1482(m), 1415(s), 1362(m), 1258(m), 1222(m), 1095(w), 1040(w), 910(m), 782(w), 696(m), 634(m). ESI-MS: m/z 474 ([Rh-((CH₃)₃CCOO)₂(N3-6-chloro-2-aminopurine)]⁺). Powder X-ray diffraction confirms the purity of the isolated solid.

In all cases, crystals suitable for single crystal X-ray diffraction studies were obtained by slow evaporation at 25 °C from the mother liquor.

X-ray Data Collection and Structure Determination. The single crystal X-ray diffraction data collections were performed at 100(2) K for 1 and 2 and at 296 K for compound 3 on a Oxford Diffraction Xcalibur (1 and 2) and on a Bruker SMART 6K CCD (3) diffractometers. All the structures were solved by direct methods using the SIR92 program⁴² and refined by full-matrix least-squares on F^2 including all reflections (SHELXL97).⁴³ All calculations were

performed using the WINGX crystallographic software package.⁴⁴ The crystal structure of compound **2** shows a very strong centrosymmetric pseudosymmetry that is broken only by the DMF solvent molecules. This pseudosymmetry correlates the anisotropic displacement parameters of the related atoms making necessary the use of soft restraints on the anisotropic displacement parameters. Crystal parameters and details of the final refinements of compounds **1–3** are summarized in Table 1.

DFT Calculations. DFT calculations on the metal complexes used Spartan Ver. Four (1.01) on a Dell Optiplex PC, at the Becke, three-parameter, Lee–Yang–Parr (B3LYP) level of theory using the 6-31g* basis set. MP2 calculations, also using the 6-31g* basis set, were performed using the Firefly QC package,⁴⁵ which is partially based on the GAMESS (US) source code.⁴⁶

RESULTS AND DISCUSSION

The compounds presented here have been obtained by direct reactions at room temperature between $[\text{Rh}_2(\text{CH}_3\text{COO})_4]$ with either 2,6-diaminopurine (HDap) or 6-chloro-2-aminopurine (HClap) (compounds **1** and **2**, respectively). In case of compound **3**, the reaction has been carried out between $[\text{Rh}_2((\text{CH}_3)_3\text{CCOO})_4(\text{H}_2\text{O})_2]$ and HClap; in all cases dimethylformamide (DMF), as solvent, and a 1:2 stoichiometric ratio was used. During the reactions the initial green solution changes to a violet suspension. This is ascribed to the coordination to the axial position of the dirhodium units of the respective purine. Electrospray ionization mass spectrometry (ESI-MS) analysis of the products agrees with the formation of $[\text{Rh}_2(\text{CH}_3\text{COO})_4(\text{N}7\text{-}2,6\text{-diaminopurine})_2]$, complex **1**, (m/z 742 ($[\text{Rh}_2(\text{CH}_3\text{COO})_4(\text{N}7\text{-}2,6\text{-diaminopurine})_2]^+$)). In the case of complex **2**, the mass spectrum (ESI) afforded a peak corresponding to the ion $[\text{Rh}_2(\text{CH}_3\text{COO})_4(\text{N}3\text{-}6\text{-chloro-}2\text{-aminopurine})]^+$ (m/z 611), and for complex **3** a peak corresponding to the ion $[\text{Rh}((\text{CH}_3)_3\text{CCOO})_2(\text{N}3\text{-}6\text{-chloro-}2\text{-aminopurine})]^+$ (m/z 474) is observed. In all three compounds, peaks corresponding to species $[\text{Rh}_2(\text{R-COO})_4\text{L}]^+$ and $[\text{Rh}_2(\text{R-COO})_3\text{L}]^+$ are observed (complex **1**, m/z 592 and 533; complex **2**, m/z 611 and 552; complex **3**, m/z 779 and 678, with $\text{R} = \text{CH}_3$ and $(\text{CH}_3)_3\text{C}$ and $\text{L} = \text{HDap}$ and HClap , respectively). Further, FTIR data show the characteristics asymmetric and symmetric O–C–O stretching vibrations of the carboxylate groups corresponding to the bridging mode at $1589\text{--}1565\text{ cm}^{-1}$ (ν_{as}) and $1423\text{--}1412\text{ cm}^{-1}$ (ν_{s}), consistent with the carboxylate groups coordinated in the equatorial position of the dirhodium units.

Crystal and Molecular Structures. Unambiguous confirmation of the structures of the isolated compounds **1**, **2**, and **3** was obtained by single crystal X-ray diffraction. The common feature of the three crystal structures is the presence of dirhodium paddlewheel units substituted in the axial positions by HDap (**1**) or HClap (**2** and **3**) (Figure 4, left). The neutral dimetallic unit consists of two rhodium atoms linked by four carboxylate bridging ligands (acetate in case of **1** and **2**, trimethylacetate in case of **3**) in an eclipsed conformation. The dimeric unit in compounds **1** and **2** are centrosymmetric whereas in compound **3**, this is not the case. However, in **3** there are no substantial differences between the two halves of the molecule; the absence of a center of symmetry is due to noncentrosymmetric packing of solvent molecules rather than to an asymmetry in the dimeric unit. Each Rh atom exhibits a slightly distorted octahedral environment with the four equatorial positions occupied by the oxygen atoms of the acetate ligands, while the fifth and sixth sites are occupied by either the other Rh-atom of the dimer or a N-donor atom from

the purine. The Rh–Rh bond lengths in complexes **1–3** are 2.4112(3), 2.3954(4), and 2.3931(6) Å, respectively. These distances are consistent with those found in other carboxylato dirhodium complexes containing Rh_2^{4+} units.⁴⁷

In all cases, the coordination of the purine to the apical position of the Rh_2 -unit is reinforced by simultaneous hydrogen bonding interactions. These involve amino donor groups adjacent to the coordination position of the purine. For example, in **1** (Figure 4, right) the coordination via N7 of the HDap to the axial positions of the dirhodium paddlewheel additionally establishes a hydrogen bond between the exocyclic $\text{H}_2\text{N}6$ -amino group and an oxygen atom of the carboxylate bridge ($\text{N}5\cdots\text{O}3 = 2.866\text{ \AA}$; $\text{N}5\text{--H}\cdots\text{O}3 = 175.8^\circ$). The HDap and the bridging carboxylate ligand to which it interacts adopt a coplanar alignment to maximize the interaction (dihedral angle = 3.4°). This N7-binding mode can be considered “typical” based on literature precedence for adenine derivatives;^{16,22} however, it is noteworthy that, to date, all such crystallographically characterized compounds feature N9-alkylation, in contrast to the N9-bound proton, as in this case.

In marked contrast, **2** and **3** contain HClap coordinated to the axial position though the pyrimidinic N3 position. Binding at the N3-purine site has only been structurally characterized once before for this type of dinuclear unit,²⁸ and in that case, steric effects of the substituent at the 6-position account for the observed binding. Interestingly, it has been proposed for the product from the reactions of $[\text{Rh}_2(\mu\text{-formamidinate})_2(\mu\text{-O}_2\text{CCF}_3)_2]$ with adenine or N6,N6-dimethyladenine.⁴⁸ It is extremely rare for *unhindered* purines, that is, derivatives that are not modified in such a way as to strongly induce such interaction, to bind at this position, as noted earlier. Indeed, Loeb’s Pd-containing macrocycle, involving coordinate and noncovalent binding of adenine (Hade), remains as one of the few well-characterized examples.^{49,50}

The cases of **2** and **3** are similar in this respect, as the N3 binding is supported by complementary hydrogen bonding interactions between the exocyclic N2 amine group and the protonated N9 position with the oxygen atoms of the carboxylate bridge. In contrast, N7 binding would yield only repulsive interaction because of the approach of the chloro substituent to the carboxylates oxygen atoms; a situation analogous to the case of guanine.¹⁶ However, further analysis reveals that rather than the, possibly expected, eclipsed orientation of the 6-Clap relative to the acetate groups of the dirhodium unit, a staggered conformation is observed (dihedral angles: 35.8° (**2**) and 41.9° (**3**)). This cannot be attributed to the steric hindrance of the methyl substituents of the 2,2-dimethylpropanoate in **3** because it also happens for the acetate bridged **2**. Therefore, there appears to be an imperfect fit between the N9/N2 hydrogen donor set and the rhodium-(carboxylate)₂ acceptor group, and indeed, the $\text{N}2\cdots\text{N}9$ and $\text{O}\cdots\text{O}$ distances are different (4.7 vs 4.1 Å). Additionally, as discussed later, an eclipsed conformation would generate too close contacts for the bond distances here. Instead, the HClap groups are rotated into the observed staggered conformation ($\text{O–Rh–N}3\text{–C}4$ dihedral angles = 29.6° for compound **2** and $35.3\text{--}38.8^\circ$ for compound **3**) and are tilted with respect to the Rh–N bond axis ($\text{Rh–N}3\text{–C}6$ angles = 165.5° for compound **2** and $168.9\text{--}172.7^\circ$ for compound **3**) in such a manner as to direct the NH groups toward *cis*-related carboxylate groups. The dihedral angle between the nucleobase and the dirhodium-carboxylate mean plane, $9.27\text{--}15.56^\circ$, also reflects this type of distortion. Other factors, such as packing forces or coordinate

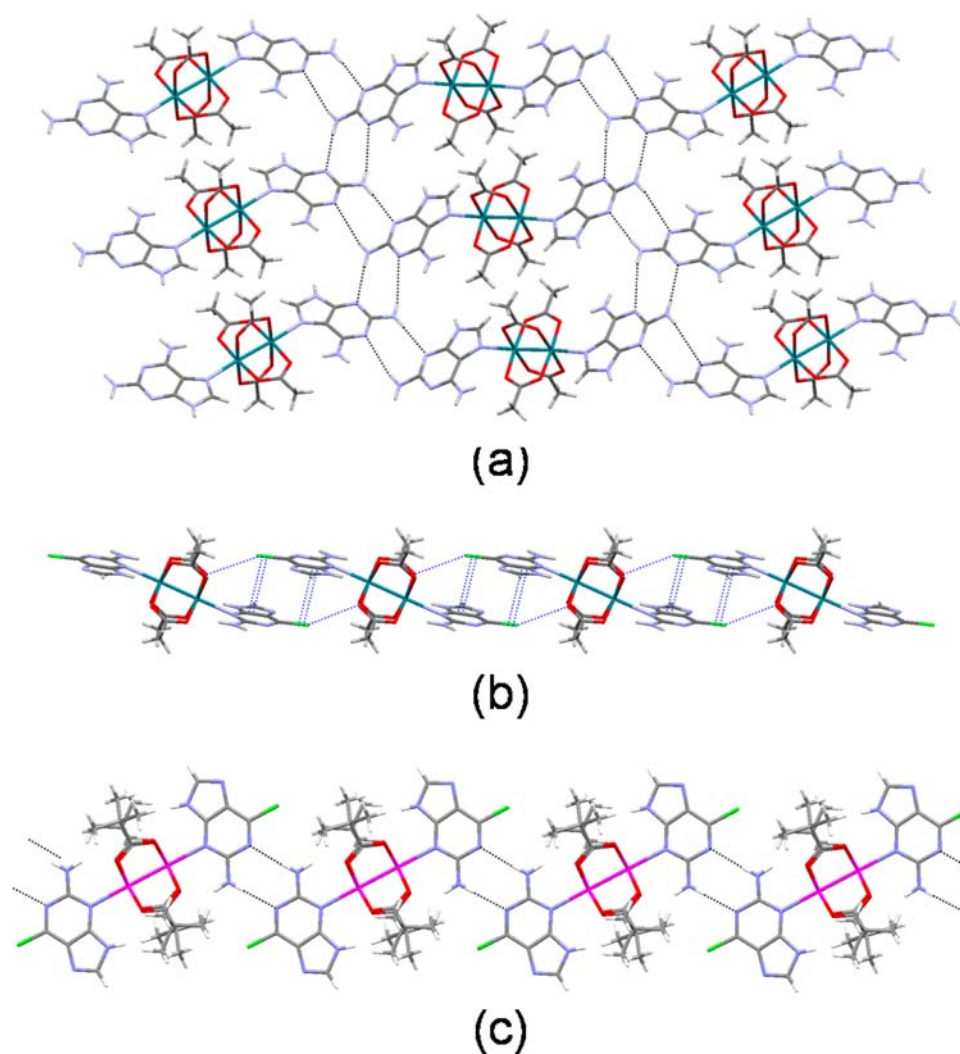


Figure 5. Supramolecular assemblies of compounds **1** (a), **2** (b), and **3** (c). Dashed lines represent interdimeric hydrogen bonds, single dotted lines supramolecular halogen Cl \cdots O bonding and double dotted ones the aromatic π - π stacking.

versus hydrogen bonding competition, may also play a role, however.

The crystal structures of compounds **1** and **3** feature direct hydrogen bonding between purine bases of adjacent molecules which give rise to infinite supramolecular motifs of the dirhodium dimers as sheets in **1** and chains in **3**. In the case of **2**, the presence of solvent molecules disrupts interpurine hydrogen bonding and instead, the dimeric units assemble into supramolecular chains by means of Cl \cdots π interactions between adjacent purine ligands (parallel distance: 3.32 Å; closest C_{aromatic} \cdots Cl contacts = 3.44–3.57 Å) (Figure 5). It is also noteworthy that supramolecular halogen bonding is observed between the chloro substituent of the purine and the oxygen atom of a carboxylate group belonging to an adjacent dimer (Cl \cdots O = 3.267 Å and C–Cl \cdots O = 154.3°; Figure 5b). This type of interaction is increasingly recognized as important in the area of crystal engineering and has also been observed in the structure of biological macromolecules.^{51–53}

¹H NMR Variable-Temperature Studies on Compound 3. The staggered orientation of the purine/carboxylate groups in the solid-state structure of **3** indicating steric constraints encouraged us to explore the solution behavior of the complex using variable temperature NMR study (Figure 6). The ¹H NMR spectra of **3** in DMF-*d*₇ at 22 °C shows a single

resonance for the C(8)-H at 8.22 ppm, as well as a broad resonance from the N(2)-H₂ group at 6.90 ppm. The signal assigned to the N(9)-H of the HClap ligand, at 11.48 ppm, is observed only at lower temperature (≤ 0 °C). Further decrease of the temperature allow the resonances corresponding to the N(2)-H₂, C(8)-H, N(9)-H protons to be observed. These signals each split into two components, consistent with two orientations of the molecule being present at lower temperatures (–40 to –60 °C). The resonance corresponding to the methyl group of the carboxylate ligand, also splits into two in this temperature range. The two forms of the molecule are present in a ratio of *approx.* 1:1.5. Similar behavior was noted for the N3-bound 6-(1-methyl-4-nitroimidazol-5-yl)thio containing complex reported by Dunbar.²⁸

These observations can be rationalized by increasingly restricted rotation about the Rh–N3 purine bond as the temperature is decreased. This leads to the molecule adopting one of two orientations. It is initially tempting to assign these two forms as being due to “staggered” and “eclipsed” orientations (*vide infra*) corresponding to weakly and strongly hydrogen bonded conformations, respectively. However, assuming an enhanced downfield shift occurs upon hydrogen bonding, such an interpretation is not consistent with the data. Specifically, the most downfield resonance for N9(H) protons

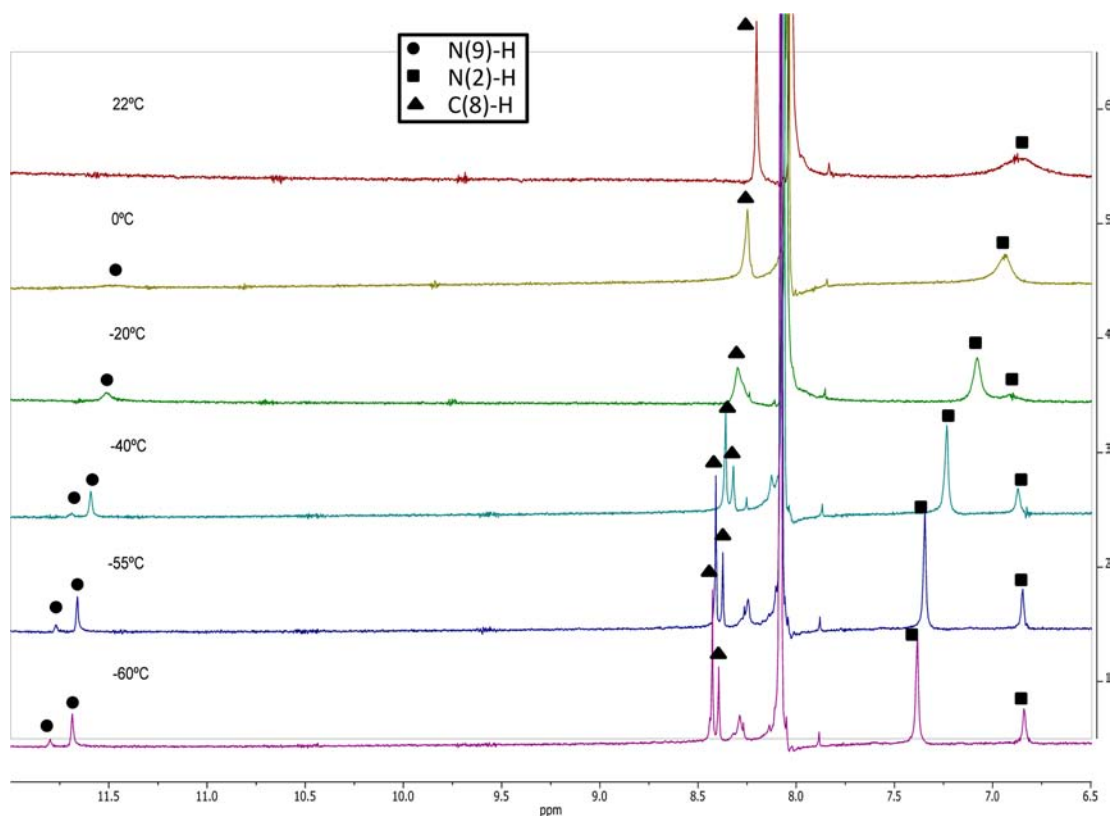


Figure 6. ^1H NMR spectra ($\text{DMF-}d_7$, TMS, low-field region only) of complex 3 at different temperatures.

corresponds to the *minor* component, whereas the most downfield N2(H) resonance corresponds to the *major* component. Such an interpretation is also somewhat at odds with the discussion of X-ray structural data above. Instead an alternative explanation is the possible formation of conformations in which the orientation of the purines relative to the Rh_2 -unit are the same sense (A in Figure 7) or in the opposite sense

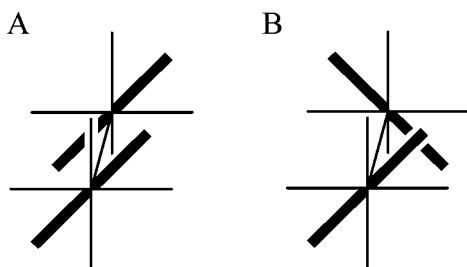


Figure 7. Two possible conformations of 3 with purines in either the same (A) or different (B) orientations.

(B in Figure 7). Head-to-head and head-to-tail conformational effects may also be involved (Figure 8) as has been previously described, by Lippert in particular, for purine-containing complexes.^{54–58} Finally, we note that there is a large temperature dependence of the resonances which means it is difficult to derive thermodynamic data on the process.

DFT Calculations. Given the apparent complementarity of the minor groove edge of the 6-HClap with regards coordinate and hydrogen bond sites on the $\text{Rh}_2(\text{CH}_3\text{COO})_4$ unit (Figure 7), the observed staggered conformation of the purines in the crystal structure of compounds 2 and 3 (angles 29.6° and $35.3\text{--}38.8^\circ$, respectively) relative to a more eclipsed geometry,

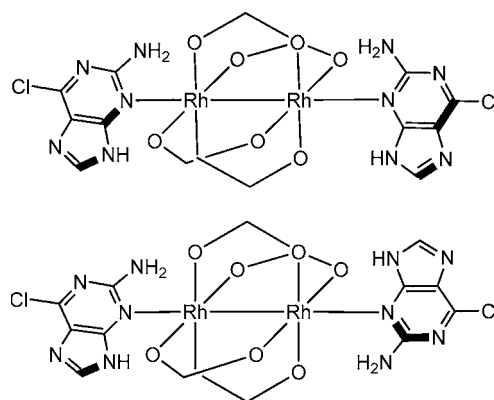


Figure 8. Upper, head-to-head and, lower, head-to-tail conformations of 3.

was intriguing. In an effort to explore the basis for this, DFT calculations were performed.

Using the crystal structure of 2 as the input starting geometry, a geometry-optimized equilibrium structure (Calc_{Eq}) was obtained and is shown in Figure 9. This has an essentially eclipsed conformation which appears to optimize the available hydrogen-bonding interactions in a manner not observed in the crystal structure. This is best illustrated by comparing several metrical parameters: N2(H) \cdots O X-ray = 2.958 \AA , Calc_{Eq} = 2.860 \AA ; $\angle\text{N2-H}\cdots\text{O}$ X-ray = 151.3° , Calc_{Eq} = 160.8° ; N9(H) \cdots O X-ray = 3.214 \AA , Calc_{Eq} = 2.773 \AA ; $\angle\text{N2-H}\cdots\text{O}$ X-ray = 123.0° , Calc_{Eq} = 148.3° ; $\angle\text{O-Rh-N3-N1}$ X-ray = -60.85° , Calc_{Eq} = -8.65° (Calc_{Eq} are the values from the calculated equilibrium geometry-optimized structure). However, further comparison of the X-ray and calculated structures reveals that the latter has markedly longer Rh–Rh and the Rh–N bond lengths (Rh–Rh

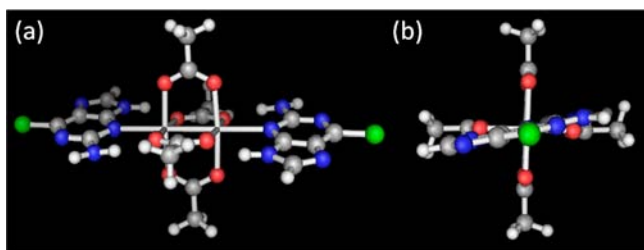


Figure 9. Geometry-optimized structure of **2** (Calc_{Eq}) highlighting the more eclipsed orientation of the purine...carboxylate interactions.

= 2.396 $_{\text{X-ray}}$, cf. 2.458 $_{\text{Calc}}$ Å; Rh–N = 2.281 $_{\text{X-ray}}$, cf. 2.429 $_{\text{Calc}}$ Å). Single point calculations ($\text{Calc}_{\text{Rotate}}$) using the X-ray structure coordinates for input, with *manual rotation* of the purines to adopt a similarly “eclipsed” conformation as the Calc_{Eq} structure are found to be less stable by as much as ~ 20 kJmol $^{-1}$. This, presumably, is predominantly a consequence of repulsive interactions brought about by the too close approach of the appropriate groups (e.g., $\text{Calc}_{\text{Rotate}}$ N2(H)...O 2.639 Å, N9(H)...O 2.556 Å, c.f. N2(H)...O Calc_{Eq} = 2.860 Å, N9(H)...O Calc_{Eq} = 2.773 Å). It may be concluded, then, that the crystal conformation of the molecule represent an appropriate balance between coordinate and hydrogen bond formation and crystal packing forces; while the orientation for hydrogen-bonding appears suboptimal, this is clearly balanced by compensating factors.

While the N3-coordination of *unhindered* purines is highly unusual, it is known that the difference between the basicity of N1 and N3 sites is often small.³² As a result, it is perhaps surprising then that more examples of unhindered N3-binding are not observed. With this in mind, we performed further calculations, at the higher MP2 level, for the purines used here as well as for adenine (Hade) and guanine (Hgua). Of particular interest was the mapped electrostatic potential, as this is considered useful for identifying likely binding sites. The data is summarized in Table 2. It can be seen that the N3-site of

Table 2. Electrostatic-Potential Fitted Atomic Charges Calculated for Selected Purines at the MP2 Level of Theory Using 6-31g* Basis Set^a

	HGua	6-HClap	Hdpa	Hade
N1	−0.8019	−0.7124	−0.7636	−0.8065
N3	−0.7757	−0.7960	−0.7727	−0.7634
N2	−1.0943	−1.0891	−1.0372	
N2H	0.4685	0.4585	0.4416	
N6		−0.0584	−0.9260	−1.0574
N6H _L			0.4259	0.4583
N6H _R			0.4225	0.4523
N7	−0.5249	−0.6116	−0.5578	−0.5763
N9	−0.5454	−0.6538	−0.5296	−0.5973
N9H	0.4067	0.4265	0.3925	0.4156

^aCalculations performed using the Firefly QC package,⁴⁵ which is partially based on the GAMESS (US)⁴⁶ source code.

HClap is the most electron-rich of the available aromatic N sites in the molecule. In fact, HClap has the most electron-rich N3 site of all the purines considered and this, along with the resulting supportive hydrogen bonding, allows a rationalization of the observed N3-binding in **2** and **3**. By contrast, an N7-bound structure (analogous to compound **1**) would lack the supporting hydrogen bonding interactions and, in fact, these

would be replaced by repulsive interactions between the electron-rich Cl...O groups.

For HDap, the N3 site charge is somewhat lower than for HClap, though it is still the most electron-rich aromatic N-site, and the difference compared with N1 is smaller. Binding at either N1 or N3, appears to offer complementary hydrogen bonding by virtue of the corresponding adjacent NH groups. Instead, however, coordination at N7 is found, as is most frequently observed for common purines. Modeling of N1-binding does show that this can give rather short distances for the corresponding NH...O interactions with, presumably, unfavorable sterics. For example, for a Rh–N distance of 2.280 Å and an eclipsed geometry the corresponding distances are; N6...O = 2.411 Å; N2...O = 2.385 Å. N7-binding however provides supportive hydrogen bonding interactions involving N6H...O_{Carboxylate} without such factors and it is noteworthy that the Calc_{Eq} geometry for **1** is remarkably similar to that found in the crystal structure [e.g., Rh–Rh X-ray = 2.412, Calc_{Eq} = 2.448 $_{\text{Calc}}$ Å; Rh–N X-ray = 2.286, Calc_{Eq} = 2.351 $_{\text{Calc}}$ Å; \angle O–Rh–N7–N9 X-ray = 2.25°, Calc_{Eq} = −6.27°]. This indicates that the geometries of the interacting groups, ligand and dimetal unit, are well matched in this case. The observed differences in the binding seen for HDap and HClap can now be understood in light of these secondary interactions and the influence of substituent on the electronic properties of the purine moiety.

CONCLUSIONS

The unambiguous characterization of N3-binding of the *unhindered* purine derivative 6-chloro-2-aminopurine to rhodium centers in the dirhodium “paddlewheel” complexes has been reported (**2** and **3**). This binding mode is supported by the complementary hydrogen bonding interactions between the purine and the carboxylate groups. By contrast 2,6-diaminopurine, despite having available the same secondary interactions to support such binding, binds in a more typical manner via N7 (**1**).

ASSOCIATED CONTENT

Supporting Information

Coordination bond distances and angles, crystal packing, and X-ray crystallographic files in CIF format for compounds **1–3** (CCDC 912677–912679). This material is available free of charge via Internet at <http://pubs.acs.org>.

AUTHOR INFORMATION

Corresponding Author

*E-mail: pilar.amo@uam.es (P.A.-O.); andrew.houlton@ncl.ac.uk (A.H.).

Notes

The authors declare no competing financial interest.

ACKNOWLEDGMENTS

This work was supported by MICINN (MAT2010-20843-C02-01, ACI2009-0969, Comunidad de Madrid (CAM2009-S2009-MAT-1467), and Gobierno Vasco (IT477-10). A.H. acknowledges Prof. William McFarlane for helpful discussions of the NMR data. P.A.-O. acknowledges Caja Madrid Foundation and Flores Valles Co. for mobility grant.

REFERENCES

- (1) Ward, M. D. *In Comprehensive Coordination Chemistry II*; Elsevier: Amsterdam, 2004; Vol. 9.
- (2) van Santen, R. A.; Neurock, M. *Molecular Heterogeneous Catalysis: A Conceptual and Computational Approach*; Wiley: Weinheim, Germany, 2006.
- (3) Cotton, S. *Lanthanide and Actinide Chemistry*; Wiley: Chichester, U.K. 2006.
- (4) Jia, C. D.; Wu, B. A.; Li, S. G.; Huang, X. J.; Zhao, Q. L.; Li, Q. S.; Yang, X. J. *Angew. Chem., Int. Ed.* **2011**, *50*, 486.
- (5) Di Pasqua, A. J.; Goodisman, J.; Dabrowiak, J. C. *Inorg. Chim. Acta* **2012**, *389*, 29.
- (6) Reedijk, J. *Metalomics* **2012**, *4*, 628.
- (7) Sun, Y. Y.; Gou, S. H.; Liu, F.; Yin, R. T.; Fang, L. *ChemMedChem* **2012**, *7*, 642.
- (8) (a) Kinoshita-Kikuta, E.; Kinoshita, E.; Koike, T. *Methods Mol. Biol.* **2009**, *578*, 169. (b) Shionoya, M.; Ikeda, T.; Kimura, E.; Shiro, M. *J. Am. Chem. Soc.* **1994**, *116*, 3848. (c) Kimura, E.; Ikeda, T.; Aoki, S.; Shionoya, M. *J. Biol. Inorg. Chem.* **1998**, *3*, 259. (d) Gasser, G.; Belousoff, M. J.; Bond, A. M.; Kosowski, Z.; Spiccia, L. *Inorg. Chem.* **2007**, *46*, 1665.
- (9) (a) Bear, J. L.; Gray, H. B.; Rainen, L.; Chang, I. M.; Howard, R.; Serio, G.; Kimball, A. P. *Cancer Chemother. Rep. 1* **1975**, *59*, 611. (b) Chifotides, H. T.; Koshlap, K. M.; Pérez, L. M.; Dunbar, K. R. *J. Am. Chem. Soc.* **2003**, *125*, 10703. (c) Chifotides, H. T.; Koshlap, K. M.; Pérez, L. M.; Dunbar, K. R. *J. Am. Chem. Soc.* **2003**, *125*, 10714. (d) Chifotides, H. T.; Hess, J. S.; Angeles-Boza, A. M.; Galán-Mascarós, J. R.; Karn Sorasaene, K.; Dunbar, K. R. *Dalton Trans.* **2003**, *23*, 4426. (e) Chifotides, T. H.; Dunbar, K. R. *Chem.—Eur. J.* **2006**, *12*, 6458. Deubel, D. V.; Chifotides, H. T. *Chem. Commun.* **2007**, 3438.
- (10) Erck, A.; Rainen, L.; Whyleyma, J.; Chang, I. M.; Kimball, A. P.; Bear, J. *Proc. Soc. Exp. Biol. Med.* **1974**, *145*, 1278.
- (11) Aoki, K.; Yamazaki, H. *J. Am. Chem. Soc.* **1984**, *106*, 3691.
- (12) Aoki, K.; Hoshino, M.; Okada, T.; Yamazaki, H.; Sekizawa, H. *J. Chem. Soc. Chem. Commun.* **1986**, 314.
- (13) Dunbar, K. R.; Matonic, J. H.; Saharan, V. P.; Crawford, C. A.; Christou, G. *J. Am. Chem. Soc.* **1994**, *116*, 2201.
- (14) Asara, J. M.; Hess, J. S.; Lozada, E.; Dunbar, K. R.; Allison, J. J. *Am. Chem. Soc.* **2000**, *122*, 8.
- (15) Chifotides, H. T.; Koomen, J. M.; Kang, M. J.; Tichy, S. E.; Dunbar, K. R.; Russell, D. H. *Inorg. Chem.* **2004**, *43*, 6177.
- (16) Aoki, K.; Salam, M. A. *Inorg. Chim. Acta* **2002**, *339*, 427.
- (17) Chifotides, H. T.; Dunbar, K. R. *Acc. Chem. Res.* **2005**, *38*, 146.
- (18) Aoki, K.; Yamazaki, H. *J. Am. Chem. Soc.* **1985**, *107*, 6242.
- (19) Aoki, K.; Salam, M. A. *Inorg. Chim. Acta* **2001**, *316*, 50.
- (20) Catalan, K. V.; Hess, J. S.; Maloney, M. M.; Mindiola, D. J.; Ward, D. L.; Dunbar, K. R. *Inorg. Chem.* **1999**, *38*, 3904.
- (21) Although there is no X-ray structural evidence for guanine reactions proceeding by axial ligand substitution, crystal structure data has been reported for $[\text{Rh}_2(\text{CH}_3\text{COO})_2(9\text{-EtG})_2(\text{MeOH})_2] \cdot 2\text{MeOH}$, where the guanine (9-EtG = 9-Ethylguanine) reacts by equatorial substitution and coordinates by bridging through N7 and O6 (ref 9).
- (22) Rubin, J. R.; Haromy, T. P.; Sundaralingam, M. *Acta Crystall. C* **1991**, *47*, 1712.
- (23) The available structural information [CSD] on the metal ions complexed by 2,6-diaminopurine (HDap) and 6-chloro-2-aminopurine (HClap) is limited to diamine-tethered 2,6-diaminopurine bound to Pd(II) and Cd(II). These complexes feature N3-binding, as a result of “directed-metallation” resulting from the chelating diamine tether. No previous reports of structures of metal-bound 6-chloro-2-aminopurine derivatives have appeared.
- (24) Meiser, C.; Song, B.; Freisinger, E.; Peilert, M.; Sigel, H.; Lippert, B. *Chem.—Eur. J.* **1997**, *3*, 388.
- (25) Pearson, C.; Beauchamp, A. L. *Inorg. Chem.* **1998**, *37*, 1242.
- (26) Sheldrick, W. S.; Gunther, B. *J. Organomet. Chem.* **1989**, *375*, 233.
- (27) Sheldrick, W. S.; Gunther, B. *J. Organomet. Chem.* **1991**, *402*, 265.
- (28) Chifotides, H. T.; Dunbar, K. R.; Matonic, J. H.; Katsaros, N. *Inorg. Chem.* **1992**, *31*, 4628.
- (29) Galindo, M. A.; Amantia, D.; Martinez, A. M.; Clegg, W.; Harrington, R. W.; Martinez, V. M.; Houlton, A. *Inorg. Chem.* **2009**, *48*, 10295.
- (30) Galindo, M. A.; Amantia, D.; Martinez-Martinez, A.; Clegg, W.; Harrington, R. W.; Martinez, V. M.; Houlton, A. *Inorg. Chem.* **2009**, *48*, 11085.
- (31) Cerda, M. M.; Amantia, D.; Costisella, B.; Houlton, A.; Lippert, B. *Dalton Trans.* **2006**, 3894.
- (32) Amantia, D.; Price, C.; Shipman, M. A.; Elsegood, M. R. J.; Clegg, W.; Houlton, A. *Inorg. Chem.* **2003**, *42*, 3047.
- (33) Houlton, A. *Adv. Inorg. Chem.* **2002**, *53*, 87.
- (34) Price, C.; Horrocks, B. R.; Mayeux, A.; Elsegood, M. R. J.; Clegg, W.; Houlton, A. *Angew. Chem., Int. Ed.* **2002**, *41*, 1047.
- (35) Gibson, A. E.; Price, C.; Clegg, W.; Houlton, A. *Dalton Trans.* **2002**, 131.
- (36) Price, C.; Shipman, M. A.; Rees, N. H.; Elsegood, M. R. J.; Edwards, A. J.; Clegg, W.; Houlton, A. *Chem.—Eur. J.* **2001**, *7*, 1194.
- (37) Shipman, M. A.; Price, C.; Elsegood, M. R. J.; Clegg, W.; Houlton, A. *Angew. Chem., Int. Ed.* **2000**, *39*, 2360.
- (38) Price, C.; Shipman, M. A.; Gummerson, S. L.; Houlton, A.; Clegg, W.; Elsegood, M. R. *J. Chem. Soc., Dalton Trans.* **2001**, 353.
- (39) Shipman, M. A.; Price, C.; Gibson, A. E.; Elsegood, M. R. J.; Clegg, W.; Houlton, A. *Chem.—Eur. J.* **2000**, *6*, 4371.
- (40) Price, C.; Elsegood, M. R. J.; Clegg, M.; Rees, N. H.; Houlton, A. *Angew. Chem., Int. Ed.* **1997**, *36*, 1762.
- (41) Rempel, G. A.; Legzdins, P.; Smith, H.; Wilkinson, G. *Inorg. Synth.* **1972**, *13*, 90.
- (42) Altomare, A.; Cascarano, M.; Giacovazzo, C.; Guagliardi, A. *J. Appl. Crystallogr.* **1993**, *26*, 343.
- (43) Sheldrick, G. M. *SHELXL-97, Program for Crystal Structure Refinement*; Universität Göttingen: Göttingen, Germany, 1997.
- (44) Farrugia, L. J. *J. Appl. Crystallogr.* **1999**, *32*, 837.
- (45) Granovsky, A. A. Firefly, version 7.1.C, 2009. <http://classic.chem.msu.su/gran/firefly/index.html>.
- (46) Schmidt, M. W.; Baldrige, K. K.; Boatz, J. A.; Elbert, S. T.; Gordon, M. S.; Jensen, J. H.; Koseki, S.; Matsunaga, N.; Nguyen, K. A.; Su, S. J.; Windus, T. L.; Dupuis, M.; Montgomery, J. A. *J. Comput. Chem.* **1993**, *14*, 1347.
- (47) Cotton, F. A.; Murillo, C. A.; Walton, R. A. *Multiple Bonds Between Metal Atoms*, 3rd ed.; Springer Science and Business Media Inc.: New York, 2005; Chapter 12, pp 465–588.
- (48) Piraino, P.; Tresoldi, G.; Loschiavo, S. *Inorg. Chim. Acta* **1993**, *203*, 101.
- (49) Kickham, J. E.; Loeb, S. J.; Murphy, S. L. *J. Am. Chem. Soc.* **1993**, *115*, 7031.
- (50) Kickham, J. E.; Loeb, S. J.; Murphy, S. L. *Chem.—Eur. J.* **1997**, *3*, 1203.
- (51) Metrangolo, P.; Resnati, G.; Pilati, T.; Liantonio, R.; Meyer, F. *J. Polym. Sci., Polym. Chem.* **2007**, *45*, 1.
- (52) Auffinger, P.; Hays, F. A.; Westhof, E.; Ho, P. S. *Proc. Natl. Acad. Sci. U. S. A.* **2004**, *101*, 16789.
- (53) Imai, Y. N.; Inoue, Y.; Nakanishi, I.; Kitaura, K. *Protein Sci.* **2008**, *17*, 1129.
- (54) Schroder, G.; Lippert, B.; Sabat, M.; Lock, C. J. L.; Faggiani, R.; Song, B.; Sigel, H. *Dalton Trans.* **1995**, 3767.
- (55) Metzger, S.; Lippert, B. *Angew. Chem., Int. Ed.* **1996**, *35*, 1228.
- (56) Schreiber, A.; Luth, M. S.; Erxleben, A.; Fusch, E. C.; Lippert, B. *J. Am. Chem. Soc.* **1996**, *118*, 4124.
- (57) Luth, M. S.; Freisinger, E.; Glahe, F.; Muller, J.; Lippert, B. *Inorg. Chem.* **1998**, *37*, 3195.
- (58) Roitzsch, M.; Lippert, B. *J. Am. Chem. Soc.* **2004**, *126*, 2421.